



## THE 20<sup>th</sup> CHESAPEAKE SAILING YACHT SYMPOSIUM

ANNAPOLIS, MARYLAND, MARCH 2011

### Experimental full scale study on yacht sails and rig under unsteady sailing conditions and comparison to fluid structure interaction unsteady models

**Benoît Augier**, Research Institute of the Naval Academy, IRENav, France

**Patrick Bot**, Research Institute of the Naval Academy, IRENav, France

**Frederic Hauville**, Research Institute of the Naval Academy, IRENav, France

#### ABSTRACT

This work presents an experimental study on the aero-elastic wind/sails/rig interaction at full scale in real navigation conditions with the aim to give an experimental validation of unsteady Fluid Structure Interaction (FSI) models applied to yacht sails. An onboard instrumentation system has been developed on a J80 yacht to measure simultaneously and dynamically the navigation parameters, yacht motion, and sails flying shape and loads in the standing and running rigging. The first results recorded while sailing upwind in head waves are shown. Variations of the measured parameters are characterized and related to the yacht motion (trim mainly). Coherence between the different parameters is examined.

In the system's response to the dynamic forcing (pitching motion), we try to distinguish between the aerodynamic effect of varying apparent wind induced by the motion and the structural effect of varying stresses and strains due to the motion and inertia. The simulation results from the FSI model compare very well with the experimental data for steady sailing conditions. For the unsteady conditions obtained in head waves, the first results show a good agreement between measurements and simulation.

#### NOMENCLATURE

AWA	Apparent Wind Angle
AWS	Apparent Wind Speed
TWA	True Wind Angle
TWS	True Wind Speed
V1	External longest shroud, from deck to top mast
V2	Intermediary shroud from deck to 2 <sup>nd</sup> spreader
D1	Internal shortest shroud from deck to 1 <sup>st</sup> spreader
I	Distance from the deck to the jib sheave
P	Distance from the boom to the top mast
J	Distance from the mast to the jib tack
E	Distance from main tack to clew
x	Center line axis in the boat reference frame
y	Lateral axis in the boat reference frame
z	Vertical axis in the boat reference frame

gyro <sub>x</sub>	Gyroscopic rotation around x axis (rad.s <sup>-1</sup> )
gyro <sub>y</sub>	Gyroscopic rotation around y axis (rad.s <sup>-1</sup> )
gyro <sub>z</sub>	Gyroscopic rotation around z axis (rad.s <sup>-1</sup> )
θ	Entry-Exit angle of a sail stripe (deg)
F	Center of rotation at the center of flotation
PSD	Power Spectral Density
G <sub>xy</sub>	Coherence of two signals x(t) and y(t)
C <sub>xx</sub>	Cross correlation of signal x(t)

#### INTRODUCTION

In the last decades, massive improvements have been made in yacht design, materials and building, as shown by the continuously increasing performances achieved by racing yachts all over the world. As yacht racing competitiveness is growing there is an increasing need for more and more detailed research and development in the field of sailing yachts. This effort yields many research activities both experimental and computational to better understand the behavior of racing yachts and to optimize their design and use. Computational Fluid Dynamics (CFD), tank testing and wind tunnel studies have been largely used to optimize hull, rig and sails design [3][2][11][18]. Concerning sails aerodynamics, many studies have been made using CFD [19] and model scale experiments in wind tunnels [9][10][13] but fewer studies have been devoted to full scale trials in real navigation conditions [5][14]. Recently, several authors have focused their interest on the Fluid Structure Interaction (FSI) problem to address the issue of the structural deformation impact on the flow and hence the aerodynamic forces generated [4][16]. The FSI problem of yacht sails is complex because the structural and aerodynamic problems are highly and non linearly coupled, and as the sails are soft structures, even small stresses may cause large displacements and shape changes leading to high variations in the aerodynamic forces. Moreover, as all sailors know, this aero-elastic problem is unsteady because of wind variations and more importantly yacht motion due to the sea state and crew actions. Very few studies have recently addressed the unsteadiness issue of sails

aerodynamics. Fossati and Muggiasca [7][8] studied the aerodynamics at model scale in a wind tunnel, and Viola and Flay[20] achieved pressure measurements on sails at full scale. To the author’s knowledge, this is the first report of experimental unsteady FSI study at full scale. Indeed, Fossati and Muggiasca showed that a yacht pitching motion has a strong and non trivial effect on the aerodynamic forces. They proved that the relationship between instantaneous forces and apparent wind deviates – phase shifts, hysteresis- from the equivalent relationship obtained in steady state, which one could have thought to apply in a quasi-static approach.

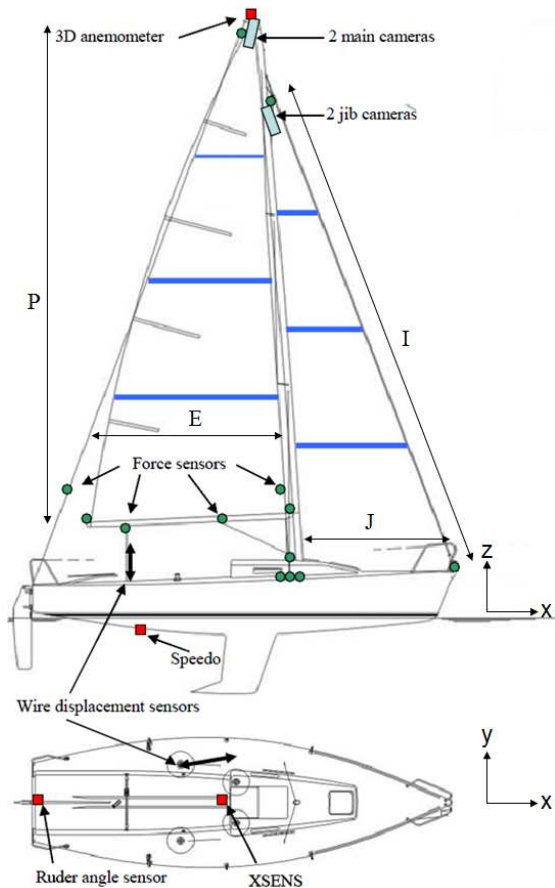


Figure 1 - Plan of a J80 with sensors general arrangement.

Table 1. Principal dimension of a J80<sup>1</sup>

HULL			
Length over all (m)			8.00
Length of water line (m)			6.71
Maximum beam (m)			2.51
Draft (m)			1.49
Disp (ton)			1.315
SAILS			
I	jib luff length (m)	9.60	9.25
P	goose neck (m)	9.14	1.26
J	E (m)	2.90	3.81

<sup>1</sup> <http://www.jboats.com/j80/j80dimensions.htm>

In this paper, the results obtained while sailing in head waves are presented and the variations of each measured parameter are analyzed and compared to the yacht motion which is the dynamic forcing applied to the aero elastic system. In the first section, the FSI model to validate is rapidly presented and the methodology developed for the experimental/numerical validation is explained. Then, the experimental system is described. The core of the paper is made of a presentation and analysis with respect to yacht motion of the unsteady recorded results: apparent wind, loads and sails flying shape parameters. In the last section, simulation results are compared to the experimental data.

### FSI MODELLING: ARAVANTI

K-EPSILON is developing a strong coupling in inviscid fluid between ARA and AVANTI, the root of ARAVANTI model. Experimental validation of ARAVANTI model is integrated in the project Voil’ENav, developed in the IRENav laboratory.

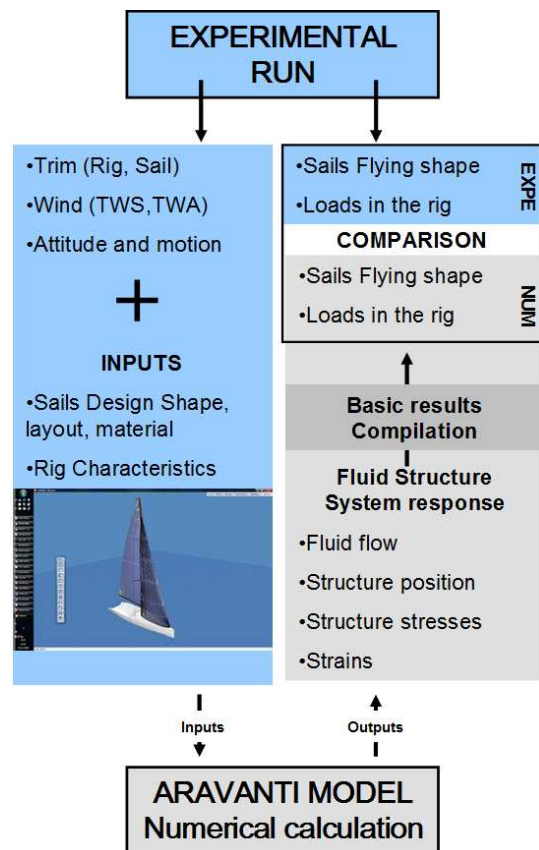


Figure 2- Methodology of the numerical/experimental comparison data.

ARAVANTI is a fluid-structure model using a CST membrane model elements extended in 3 dimensions [17]. The assumptions imposed inside this element are constant

stresses, constant strains and uniform stiffness of the material. Non-linearities coming from the geometry and compressions are taken into account. The calculation of the flow around the sails is carried out under the assumption of an incompressible inviscid fluid, using a particles method developed by Rehbach [15] and then Huberson [12]. This method is in essence unsteady, taking into account the sleep condition on the surface as a boundary conditions. A Kutta-Joukowski condition is imposed on the trailing edge of the sail, initiating the wake of the flow. An atmospheric wind gradient is taken into account. The effects of the interaction are translated into a coupling of the kinematic equation (continuity of the normal component of the velocity at the interface between fluid and structure geometrical domains) and dynamic equations (continuity of the normal component of the external force, pressure forces, on the contact surface of the sail with the fluid).

In order to validate the model, two experimental settings have been developed, dedicated to FSI measurements on soft surfaces. The first experimental system is the instrumented sail boat, subject of this paper, which is adapted to full scale and real condition study. The second system is a laboratory experiment consisting in a swiveling sail which has been described in a previous paper [6]. It represents a good test case for the FSI issue on soft surface, without the onboard instrumentation problems and a well controlled environment.

Figure 2 presents the Experimental and Numerical validation loop for the instrumented boat set up. ARAVANTI settings are given by the trim, the wind vector and the yacht attitude recordings. Rig and sail geometry and mechanical characteristics are added as inputs. Calculation results are compared to the loads and flying shapes measured on navigation.

## EXPERIMENTAL APPARATUS

Full-scale measurements were performed on a J80 yacht, an 8.00m cruiser sport boat. Principal dimensions of the J80 are presented in Table 1. A dedicated instrumentation has been developed in order to measure the unsteady navigation loads, flying shape and navigation parameters. Figure 1 shows the general arrangement of the boat.

Loads measurement is performed by instrumented fittings with stress gauges. Seven instrumented turnbuckles measure the six shrouds loads and the forestay and eight instrumented shackles are shared between the different tension points of the mainsail (outhaul, sheet, halyard, cunningham and boom vang) and the Jib (sheet, halyard and tack). A ninth shackle is placed on the backstay. The 16 load sensors are connected to two Spider8 analog data acquisition and synchronization devices from HBM inside the boat.

Four analog cameras are fixed on the mast, two on the real top recording the mainsail and two under the forestay hound point recording the jib. For measuring convenience, horizontal stripes are drawn on mainsail and jib at height of 20%, 40% and 70% of luff length. Sail shape parameters are extracted manually from pictures by image processing software ASA and ISIS as shown in Figure 4. Sail shape parameters are defined on Figure 5. Calibration grids are placed on the deck to adjust the cameras position and angle during post processing [21]. Additional cameras are fixed on the roof recording the crew and the sail foot.

Sails recorded in experiment are designed by the sail maker Delta Voiles and used in the J80 class International championship. The mainsail is half batten with the highest in full batten. The jib gets a half batten on top and two roller battens. Figure 3 shows the sails geometry. The sail maker CAD SailPack® from BSG Development is used to design the sail (design shape, cloth panel type and orientation). ARAVANTI is coupled to SailPack® in order to build the sail structure meshing from the CAD. Sails dimensions are presented in Table 1, where I, J, P, and E are the measurement lengths of sail dimensions according to the IMS rules.



Figure 3- Representation of the sails geometry with battens and frames from CAD SailPack®

The Motion sensor Xsens MTi-G is placed on the point F, the rotation center of the hull for the small angle at 0° heel angle. An ultrasonic 3D anemometer is fixed on the top mast and a speedometer has been installed on the J80 hull. Wire displacement sensors are fixed between the main

car and the boom and the jib car and the clew to measure the sheet length. A rudder angle sensor is fixed on the helm basis. A fluxgate compass and a GPS are used inside the boat.

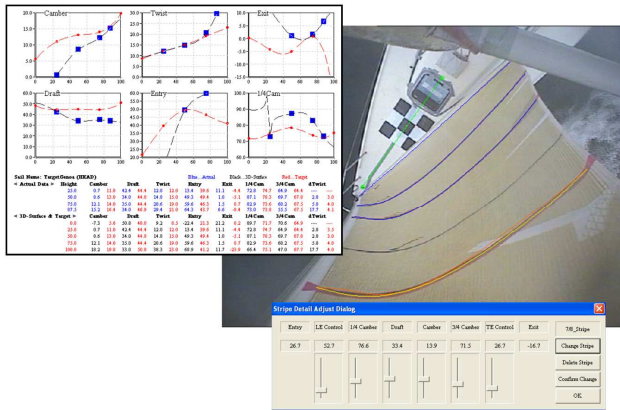


Figure 4- Example of a stripe parameter image processing on the Jib with ASA software

Sensors are linked to an onboard PC. Acquisition is controlled by RTmaps®, a dedicated software for synchronization and dating developed by Intempora.

The general arrangement and calibration method for the instrumented J80 were described in more detail in a previous article [1].

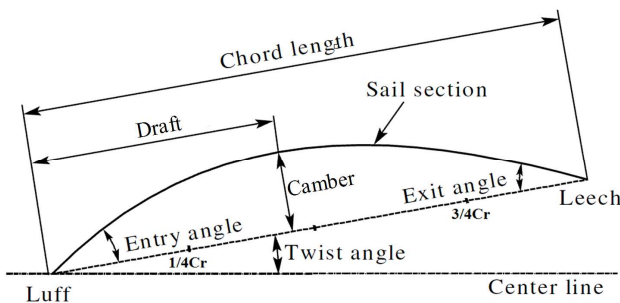


Figure 5- Definition of the flying shape parameters

## RESULTS

The data acquisition system, using RTmaps, is based on the principle of associating the events' date to each recording. Sensors are free to communicate to the computer at their own frequency and the output is dealt by the buffer. A logfile is built chronologically with the date of record in the hard disk. The frame contains the creation date of the measurement and can be extracted in post processing. The unprocessed data measurement matrix is aperiodic and gets several values for the same date. Data presented in this article have been sampled at 50Hz.

The low frequency experimental data, from NMEA frame, used as inputs to the computations, as the loch speed, the GPS speed or the fluxgate compass heading, have been smoothed to avoid jumps which would input irrelevant noise in the simulation.

## Presentation of data

### Unsteady data

This section is focused on the recordings made on a 35 second run of pitching in head swell with 20s of special interest for comparison. The swell is short with an average period of 1.3s and 0.3m wave height. The variation of the trim, the heel, the heading angle and the boat speed is presented figure 6. Heading are recorded by the Xsens motion sensor and the compass. Boat speed is recorded by the loch. The bound of the 20s of interest are pointed by the vertical lines marked by *START* and *END*. The boat is sailing on port tack. The boat speed recorded by the loch and the heading recorded by the fluxgate compass is presented on Figure 7. There is no information on the jib tack because the shackle was broken at the beginning of the experimental set.

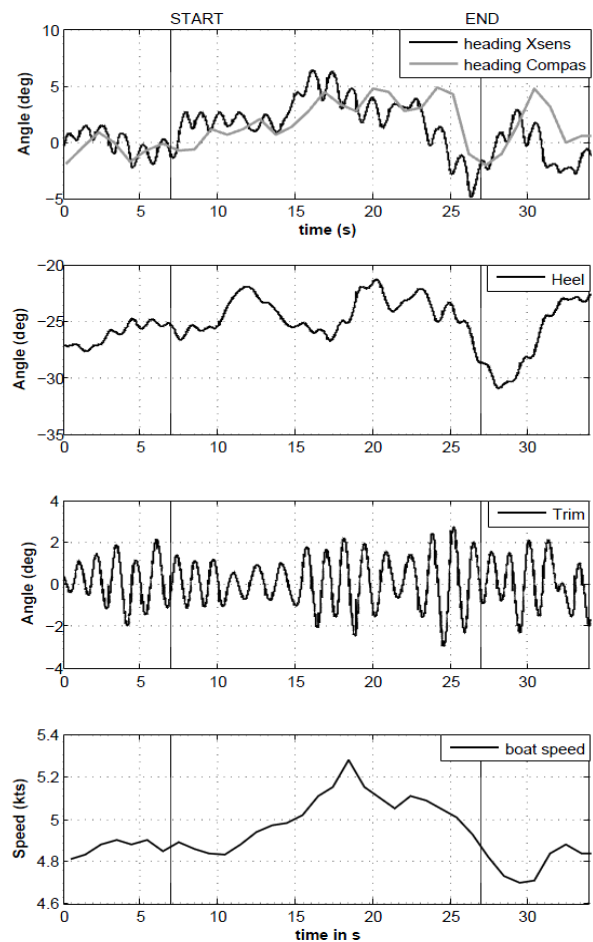


Figure 6 –Variation of heading angle, heel angle, trim

angle and boat speed in head swell on a 35 s run.

According to the reference frame adopted for the boat and presented in Figure 1, positive values of the trim correspond to the boat diving.

Figures 7 and 8 present the effect of pitching on sail loads, trim angle, and apparent wind angle and speed. The recorded run, containing the 20s of interest between bounds, is represented on 35s.

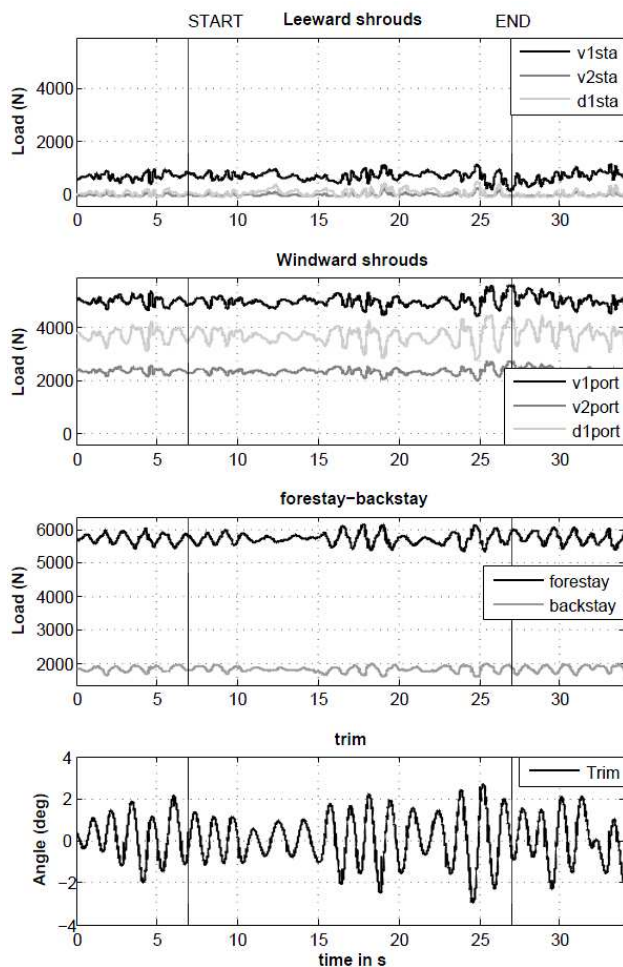


Figure 7 – Loads in shrouds during 35s.

Loads in shrouds appear to be sensitive to trim angle and the pitching oscillations are contained in the loads variations. Amplitude of variation seems to be related to the load level. In fact, Windward shrouds are more sensitive to boat oscillation than leeward ones. The same conclusion can be made on the proportionality of efforts with forestay and backstay. D1portside has the biggest variation amplitude. D1portside has an important longitudinal component of effort which is added to the

wind variation.

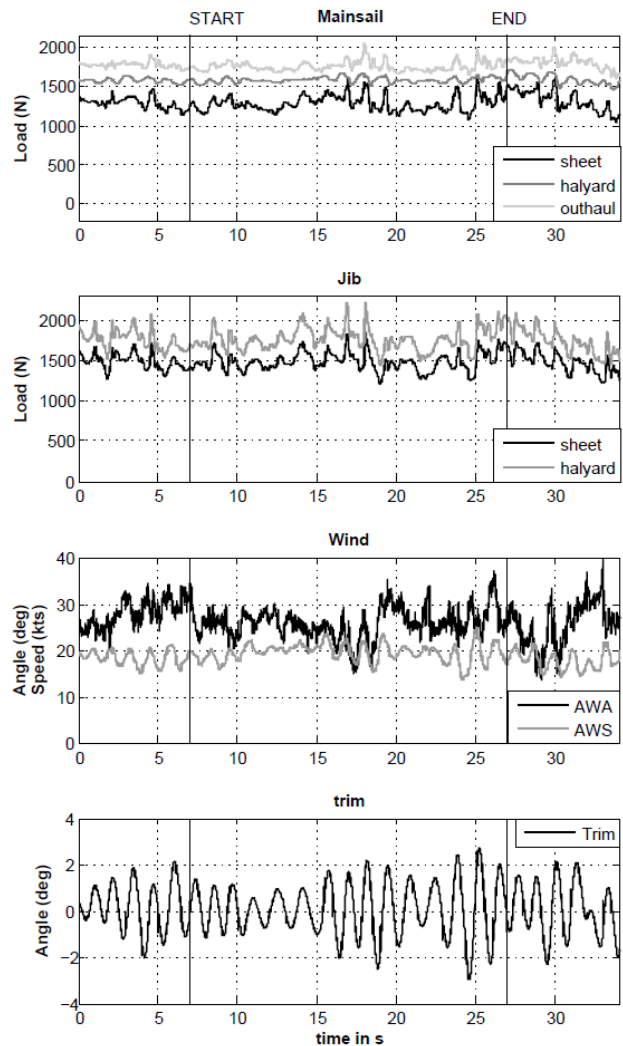


Figure 8– 35s time history of loads in mainsail and jib; apparent wind angle and speed; trim angle.

Loads in sails are also sensitive to pitching with an important relative variation due to oscillation. Mainsail outhaul and Cunningham are not represented here for legibility reason but get the same sensitivity to oscillation.

Oscillations of apparent wind angle and speed seem to be linked to the pitch. Because of head swell, oscillations on the top mast create a longitudinal component of speed. Depending on the direction of pitching, this component is added or subtracted to the apparent wind speed. This pitch speed on top mast component has an influence in AWA, illustrated in the signal oscillation fitting the trim. AWA is also sensitive to the other motion parameters, especially the yaw, reasons for the important variations.

#### Amplitude of variation due to pitching

As showed in last paragraph, loads and winds are

pitch sensitive. For loads, the amplitude of variation depends of the initial value and direction of effort (longitudinal component of effort is more sensitive to structure oscillation). Considering the aeroelastic response of the system to the unsteady forcing due to the sea state, two types of behavior can be distinguished. The effects of this behavior can be put in two groups:

- The structural group: Boat motion is dominant in the behavior.
- The wind group: Varying AWA and AWS, induced by boat motion, is dominant. The behavior is linked to the aeroelastic behavior.

The structural group is directly sensitive to the trim oscillation. The wind group is sensitive to the wind oscillation. Pitching period can be found in signals because the apparent wind is linked to oscillation. The Wind group signals have much more oscillation because the wind plays the role of a system response to the trim.

Maximum amplitude of variation of sailing parameters during the unsteady 20s is presented in Table 2. Maximum variation is defined as:

$$\Delta Max = \max[(\bar{u} - \min(u)) \cup (\max(u) - \bar{u})]$$

Table 2– Amplitude of variation due to pitching

	Mean	Max	$\Delta Max$	$\Delta Max\%$
<b>Shrouds</b>				
V1port(N)	4993	5618	625	12.5
V2port(N)	2363	2749	387	16.6
D1port(N)	3710	4487	778	20.9
forestay(N)	5724	6155	431	7.5
backstay(N)	1850	2006	156	8.4
<b>Mainsail</b>				
sheet(N)	1274	1603	329	25.8
halyard(N)	1566	1718	152	9.7
cunningham(N)	383	478	95	24.8
boom vang(N)	1709	1890	181	10.6
outhaul(N)	1758	2046	288	16.4
<b>Jib</b>				
sheet(N)	1479	1836	357	24.2
halyard(N)	1752	2214	462	26.4
<b>Wind</b>				
AWS(kts)	19	25	6	34.2
AWA(deg)	27	40	13	48.9

Wind group has higher variation in amplitude by 15-25% because the influence of trim is modified by the AWA and AWS variation. The wind filter exaggerates the effect of pitching. Structural group variation amplitudes are lower than 10%.

### Pitching frequency signature

As shown on Figures 6, 7 and 8, the pitching

oscillation appears in the different parameters time series. Figure 9 shows the Power Spectral Density (PSD) of the trim, the V1portside and the AWS signals. The PSD is the Fourier transform of the autocorrelation function,  $C_{uu}(\tau)$ , of the signal  $u(t)$ .

$$PSD(f) = \int_{-\infty}^{\infty} C_{uu}(\tau) e^{-2\pi i f \tau} d\tau = F(C_{uu}(\tau))$$

$$C_{uu}(\tau) = \int_{-\infty}^{\infty} u(t) \cdot u(t - \tau) dt$$

Where  $F(C_{uu}(\tau))$  is the continuous Fourier transform of the auto correlation function  $C_{uu}(\tau)$ .

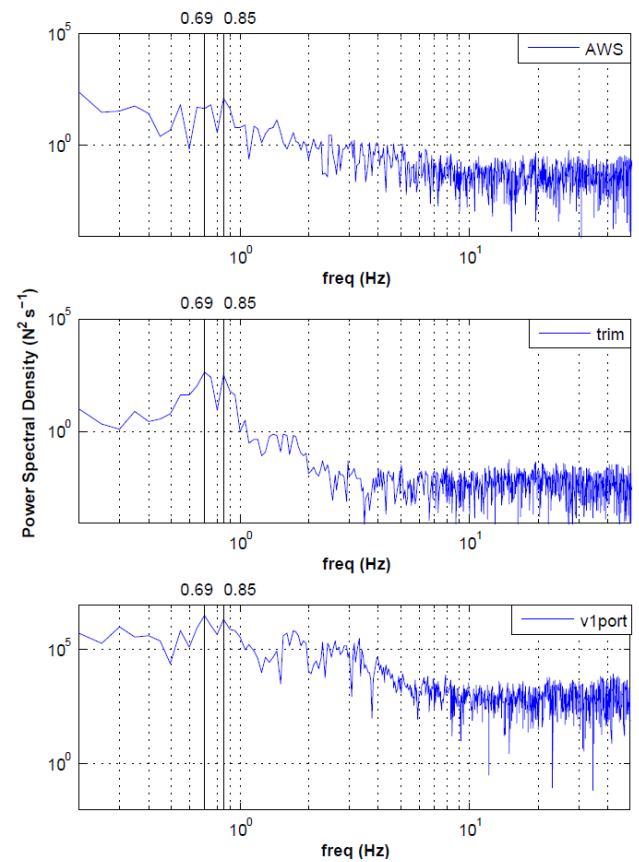


Figure 9 – Power Spectral Density of the AWS, trim and V1portside signals with logarithmic scale.

Graphs are represented in logarithmic scale. The PSD of trim shows that the trim oscillation has 2 frequencies very close: 0.69Hz and 0.85Hz. Those 2 frequencies can be explained by the 2 different swell periods encountered during the 20s run. The PSD of AWS and V1portside contains those frequency peaks. This representation confirms that the pitch oscillation is present in loads and apparent wind. Peaks can be found in the PSD of all load signals and AWA. The V1 portside is more subject to high frequencies, which is a signature of structural dynamics.

### Signals temporal coherence

Two temporal signals are said to be coherent if they have a constant relative phase. The coherence quantifies how correlated are the signals. It may be interpreted in terms of cause-effect relationship. The cross-correlation quantifies the ability to predict the value of the second wave by knowing the value of the first.

With  $C_{xx}$  the auto correlation of the time series  $x(t)$  and  $C_{xy}$  the cross correlation of signals  $x$  and  $y$ , coherence  $G_{xy}$  of times series  $x(t)$  and  $y(t)$  is:

$$G_{xy} = \frac{C_{xy}}{C_{xx}(0).C_{yy}(0)}$$

Coherence matrices of measured data have been calculated in order to identify the temporal coherence. The maximum coherence value is 1. Maximums of the absolute value of coherence have been plotted in Figure 10. This representation is a first and quick approach to highlight the coherence between signals. The white diagonal (maximum of coherence function=1) represents the auto correlation. The auto correlation diagonal is the symmetry axis of the graphic.

Coherence is important between the shrouds signal, especially the V1portside and starboard. Backstay and forestay are also coherent. Trim is coherent with forestay and backstay loads, gyro<sub>y</sub> and gyro<sub>z</sub>. Main sheet is coherent with outhaul.

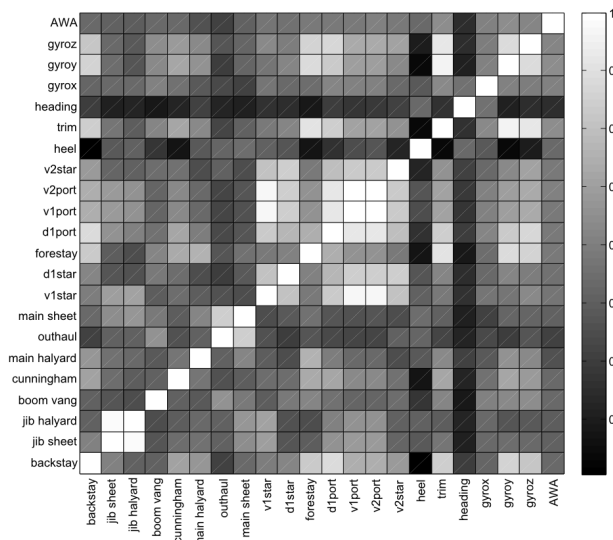


Figure 10 – Graphical representation of the maximum of the normed coherence of signals between each other.

This first approach finds some coherence between the recorded parameters. The plot of the coherence function, as in Figure 11 in the case of trim and backstay, gives information about the nature of coherence as in-phase or phase opposition (sign of the maximum of coherence) and

the phase shift (abscissa of the maximum coherence). The maximum coherence is highlighted by a black square in the graph. The signals have a positive coherence of 0.84 which indicates good correlation. The maximum coherence appears for  $t=0.25s$ , which indicates a 0.25s phase lag of backstay load oscillation.

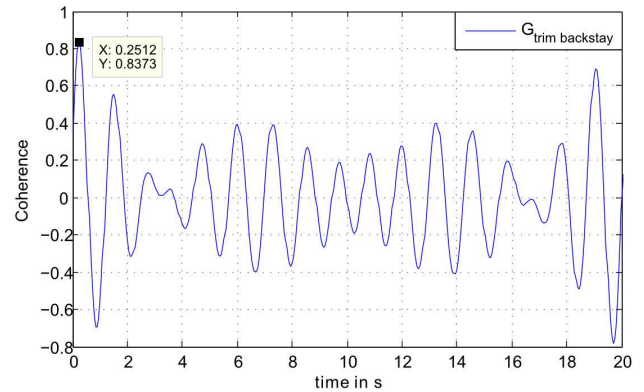


Figure 11– Coherence between the trim and the backstay measured signals with a wrap around order. The maximum coherence value is 0.8373 with a phase shift of 0.25s.

Coherence information is summarized in Table 3 for D1portside coherence with other signals. V1 and V2 portside are precisely in phase with D1 signals. Pitch is in phase advance and V2stbdside is in anti phase with a little phase shift late.

Table 3– maximum coherence and phase shift of D1portside with navigation parameters

Coherence with D1port		
signal	max coherence	phase shift
V1port	0,924	0s
V2port	0,914	0s
V2star	-0,794	-0.08s
pitch	0,850	0.12s

### Navigation parameters comparison

To isolate the unsteady behavior, the mean value is subtracted from the data times series and we define:

$$\Delta u(t) = u(t) - \bar{u}$$

$$\text{Where } \bar{u} = \frac{1}{T} \int_0^T u(t) dt$$

With  $u$  a measured signal depending on time.

### Influence of the trim on navigation parameters

The trim angle is a way to observe the pitching effects on the navigation parameters and the dynamic effects on loads in the rigging. The frequency of the pitch oscillation can be found in the temporal representation of

the load in the shrouds as presented in Figure 13. The phase shift is explained because AWS is directly linked to the gyroscopic motion around y axis. Trim angle is the integral of gyro<sub>y</sub>. AWS peaks correspond to trim(t) maximum slope. As the apparent wind is measured on the top mast and the motion is recorded on the point F of the hull a phase shift may also be caused by deformation of the mast.

The dynamic response of the boat is sensitive to short amplitude pitching. The maximum variation presented in table 2 gives an over speed of 34% for the AWS and an over loads of 21% for the D1portside. Temporal representation, with the light of frequency and coherence study, is a reliable tool to have a global idea of the load variation in the rig. It is relevant that the stationary hypothesis used in simulation or VPP for the apparent wind speed is quickly not realistic.

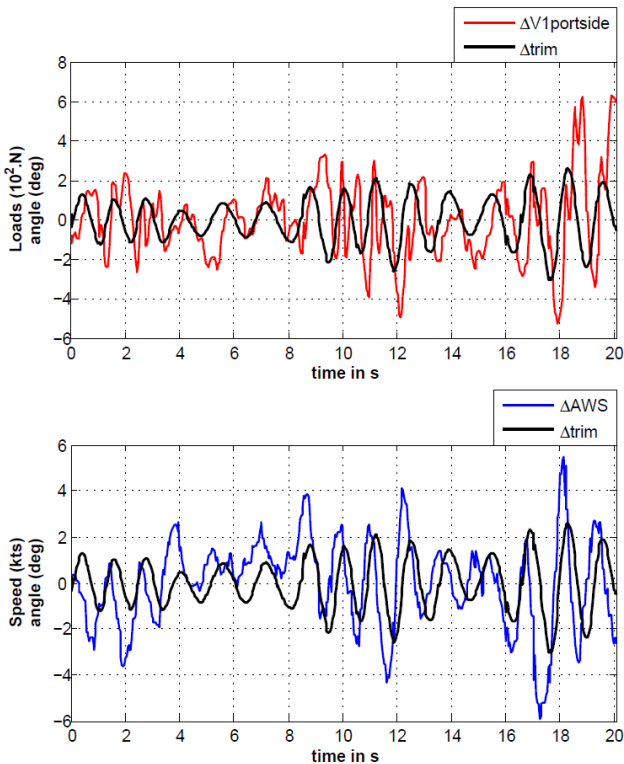


Figure 12 – Variation of  $\Delta$ load in V1portside and  $\Delta$ speed of apparent wind regarding to the trim.

### Influence of the AWS on loads in the rig

The AWS depends on the trim as illustrated in the last paragraph. The variation of AWS due to pitching has an influence on the sails performance. Figure 13 shows the temporal evolution of loads in the shroud V1portside and the forestay, while Figure 14 deals with loads in mainsail and jib sheets superposed on the AWS. All these parameters are in the Wind group.

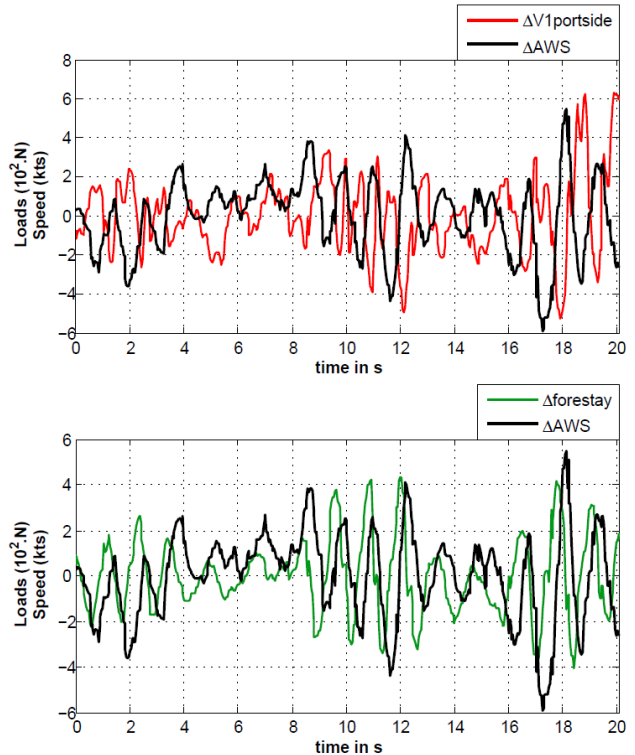


Figure 13 – Temporal evolution of the  $\Delta$ loads in shrouds compared to the  $\Delta$ AWS variations.

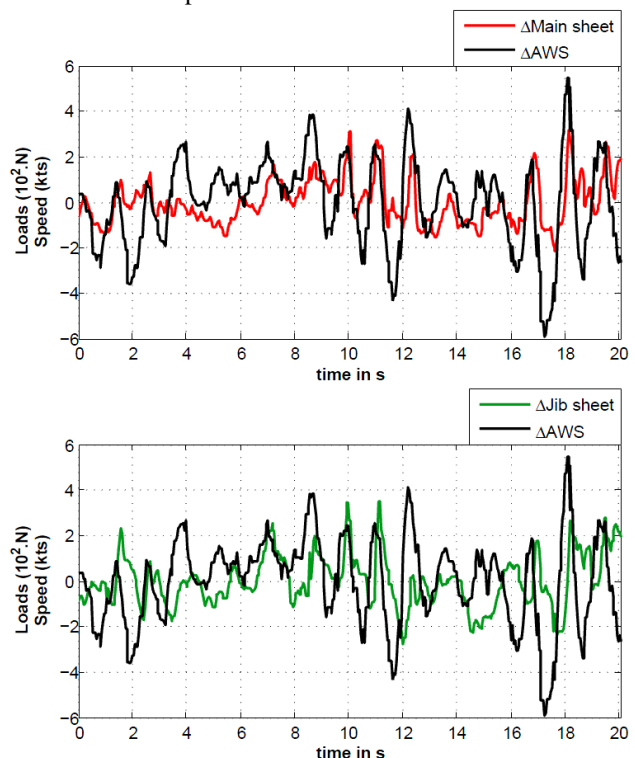


Figure 14 – Temporal evolution of the  $\Delta$ loads in sails sheets compared to the  $\Delta$ AWS variations.

Oscillations and load peaks fit to AWS signal in the case of sheets. The tension in sail seems to respond immediately to the apparent wind puff in the 10 last

seconds of run. Wind speed decreases have less influence on the load. Main sheet loads is totally coupled to AWS and suffers over loads up to 25% when the over load of jib sheet is 24%.

Shrouds loads seem less connected to the variation of AWS regarding the figure 13. The principal wind peaks are followed by an increasing load in forestay but the general signal appearance is quite different. Pitching periods can be identified in the last 12sec for the forestay. Maximum peaks represent 7.5% of the average load.

Influence of the unsteady effects and the consequences on loads in shroud and sail tension points is obvious in this temporal representation. Those phenomena underline the importance of an unsteady model to simulate the flow and the stress in sails.

### Load hysteresis during pitching

Pitching has an influence on the variation of the load in the rig as presented in previous figures. The study of the influence of trim on loads gives not only information about dynamic behavior and peak loads but also on the hysteresis phenomenon.

Figure 15 presents the variations of the forestay, main sheet and backstay load during pitching. The two runs represented correspond to two different complete periods of oscillation. Forestay and backstay load variations are elliptical. Reading direction is indicated by an arrow.

The hysteresis loop denotes the presence of a phase shift between loads and the pitch. If loads were perfectly in phase with the trim angle variation, the hysteresis loop will appear as a simple line. The simple line is the representation of the steady state trend. Depending on the sign of the phase shift, the area inside the loop represents the amount of energy that is dissipated by the head swell pitching or added to the rig and sails.

The negative slope of the forestay loop indicates that the forestay and trim signal are in anti phase. Because forestay is late to trim, the area in the loop represents the energy added by the head swell in the rig

The backstay hysteresis loop is nearly horizontal (zero slope) indicating that backstay and trim have a  $\pi/2$  phase shift.

Main sheet hysteresis variations are concentrated between 0 and +2 deg of trim, like if the sheet was pulling the sail back during positive pitching. The tendency is a positive slope, meaning that main sheet is in phase with a late phase shift with trim signals.

### Unsteady sails flying shape

Video frame grabbers have a low acquisition rate and the frame rate is different from a camera to another. Jib pictures are recorded around 6.5 Hz and mainsail pictures are recorded around 3.4Hz on portside tack.

Sails parameters have been extracted from the picture

of sails, taken from the top mast. Sail analysis produces a great amount of results. Only 4s of the Jib parameters will be presented. Jib pictures are the 21 last. The 70% stripe as the highest is the closest to the camera and gets the best resolution.

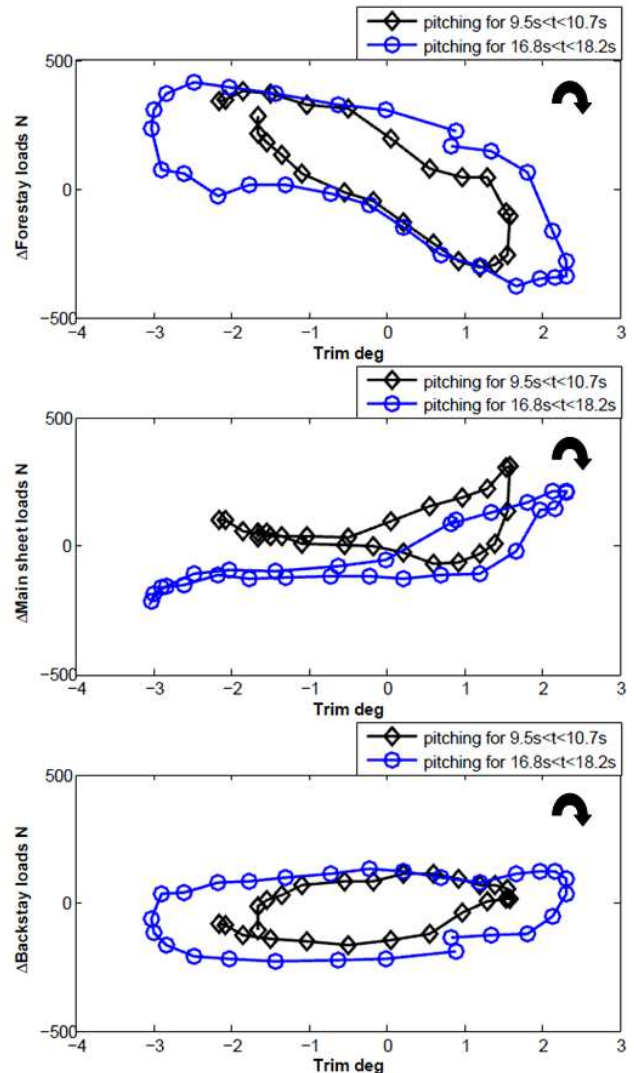


Figure 15 – Loads variation during pitching periods

Because of the higher frame rate, the jib parameters can be presented graphically. Figure 16 presents the variation, around the mean value, of the principal sail parameters, defined on Figure 5, at the 70% stripe. Parameters are linked with another measured signal in order to present their influence.

Jib halyard and sheet load variations appear to have to play on the difference of angles of entry and exit,  $\theta$ . A bigger  $\theta$  increases the camber and makes the draft moving forward, closer to the luff. Trimmers commonly adjust the halyard tension to change the sail profile. An augmentation of loads has the consequences of decreasing the thickness of the sail profile and moving forward the draft. Figure 17 confirms this tendency.

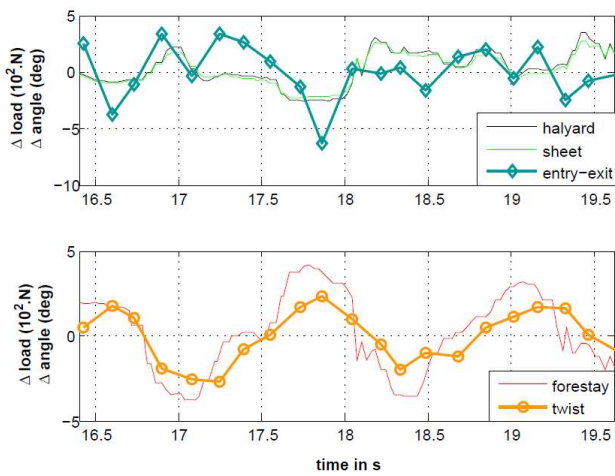


Figure 16 – Variation of 70% Jib stripes parameters regarding loads in Rig and trim oscillation.

Variations of loads in forestay are put in relation with the twist. An increase in forestay load decreases the sag. The influence is decreasing the camber and increasing the twist. The pitching oscillations in loads put into evidence in the last paragraphs are present in the twist temporal evolution. The increasing load in the forestay opens the top of the sail, meaning it increases the twist angle.

The draft variation seems in a first approach to be linked to the trim. The period of trim can be read on the signal with a phase shift. Because inverse tendencies should be observed on draft variation, the image processing on camber position has been tested. The result of this test indicates that the variations observed are closed to the precision error and cannot be taken into account.

Picture resolution and image processing tools are limited. Small variations are hard to identify, the difficulty increasing with the stripes and camera distance. The trends observed on the 70% jib stripe are not obvious for the lower stripes. Figure 17 presents the superposition of the 3 stripes camber, twist, draft and  $\theta$  with the trim temporal evolution. Mean value have been subtracted from the data. Only the twist angle confirms the periodic evolution linked to pitching. The other parameters suffer from picture resolution and post processing precision. A simple visual estimation of the parameters from the pictures is consistent with the evolution experienced sailors would expect.

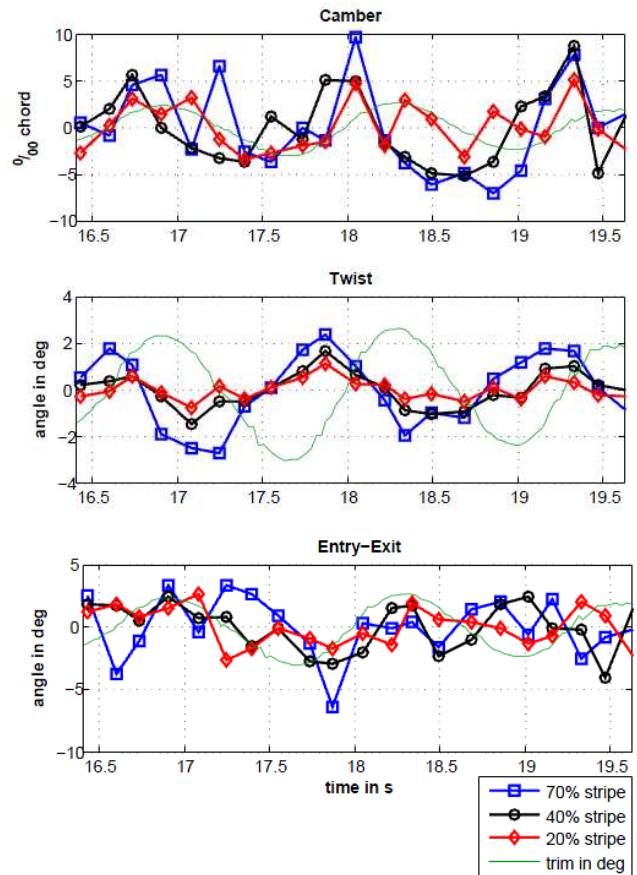


Figure 17 – Variation of the 3 Jib stripes parameters, (70%, 40% and 20%) regarding trim oscillation.

## NUMERICAL AND EXPERIMENTAL COMPARISON

### Steady state

In order to start the validation and to give relevant information to the ARAVANTI model before starting an unsteady calculation, a steady state is studied. A 10sec run was selected because of the few variations and the static loads and navigation parameters. The boat is navigating on port tack in close haul. Experimental data of the different parameters defined as inputs, shown in Figure 2, are given to the model: average value on 10sec of the trim of the rig and the sail, TWA and TWS and boat attitude. Only attitude, heel, trim and heading are imposed to the code. Motion, roll, pitch and yaw are not inputs, they are calculated from derivative of attitude. Sails design shape, layout, material, rig mechanical characteristics are frozen model inputs for all J80 fluid-structure modeling.

Figure 18 presents the numerical and experimental comparison of the loads of the instrumented sail boat based on the mean values calculated from the steady state. Trimming is adjusted to fit to the tension. Loads in sail

tension points are very well evaluated. Simulation predictions fit the measured value in the case of jib sheet and halyard, main halyard and sheet, outhaul, and boom vang. The cunningham is working in the low part of the sensors range, which can explain the discrepancy between measurement and prediction.

Loads in the shrouds are also well predicted, especially for the backstay and the windward shrouds. Prediction is given with a relative error <8% for the windward shrouds. Leeward shroud loads are quite difficult to compare because of their very low values. Forestay simulation fits to experimental data within 10% relative error. Thus, we can consider that the model reaches the goal by respecting the experimental trends and by giving good estimates.

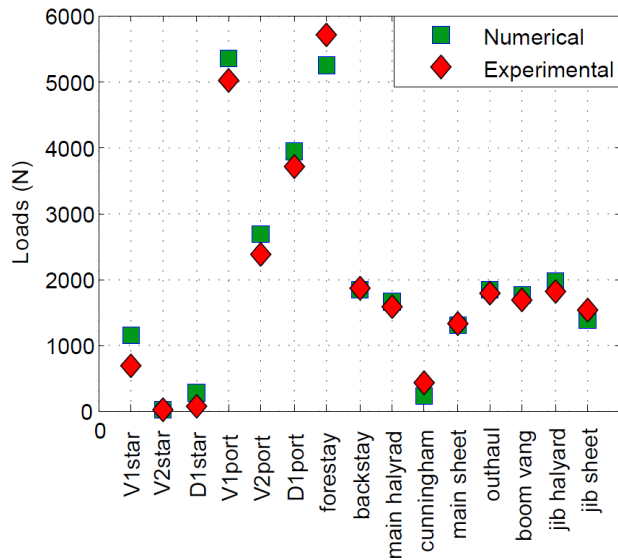


Figure 18 – Experimental and numerical comparison on loads for a steady state run of 10s.

ARAVANTI model gives a graphical representation of the calculation in order to appreciate the simulation on the flying shape. Superposition of the numerical result with the recorded picture of the sail in navigation allows going forward with confidence than the realistic feeling coming from the simulation.

Figure 19 shows the superposition of the calculated flying shape of the sails for the steady state and the recorded sails shot during the 10s run. Main sail calculation is presented with the stresses in the sail cloth in color scale. Calculated sails shape match very well the recorded one, stripes fitting nicely between each other. The camber is well predicted and the draft position is placed correctly. The twist seems also ok. The experimental jib was modified and the top batten was changed, which explains the angle in the picture. Rig and boom calculated fit very well to the picture as the blue superposition shows.

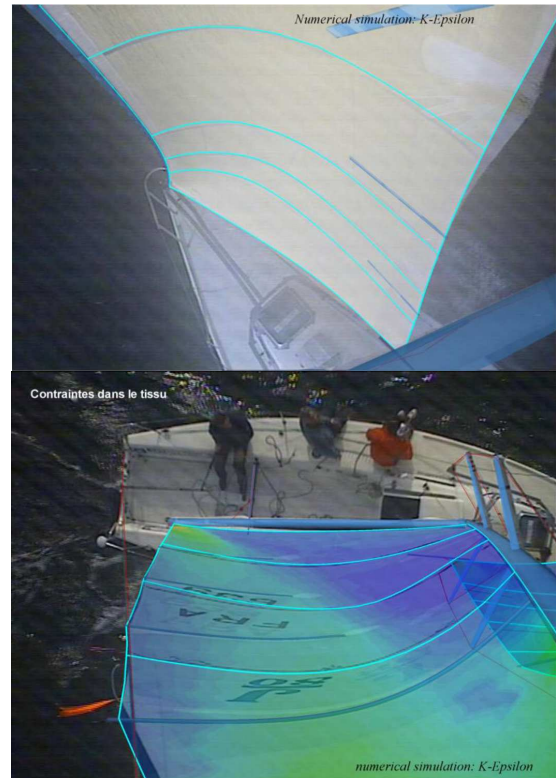


Figure 19. Comparison of the experimental flying shape (dark blue stripes) and the numerical result (bright blue) on a port tack close hauled steady state. Experimental stripes are hidden under the computed ones

### Unsteady state

A 20s run of pitching in a head swell on a port tack has been chosen for an unsteady calculation. A steady state calculation made on 5 sec, with parameters recorded just before the pitching, has been made in order to launch the simulation with the right loads and attitude. During simulation, boat is navigating on a constant wind of 14knots, with a heading to North (0deg) with a TWA on NW (320deg). Recorded variations of AWA and AWS are supposed to come only from the boat motion. Recorded attitudes, from Xsens motion sensors, are implemented as inputs. Signals are resampled at 200Hz and then smoothed in order to get a continuous second order derivative. Heading has been shifted, considering the simulated TWA, in order to start with the same configuration. Calculation is made with time step of 0.05s.

### Results

Primarily results are presented in Figures 20, 21, and 22. The same representation criteria used in experimental results are adopted in order to compare the signals.

Figure 20 presents the evolution of the  $\Delta$ loads in

the forestay superposed to the trim during the 20s of pitching. Experimental and numeric  $\Delta$ loads are represented. Variation tendencies are the same, simulation representing well the oscillation. Amplitudes of variation are a little bit over estimated when the pitch solicitation gets higher. It seems that the computed boat is less limited in this motion than the real one.

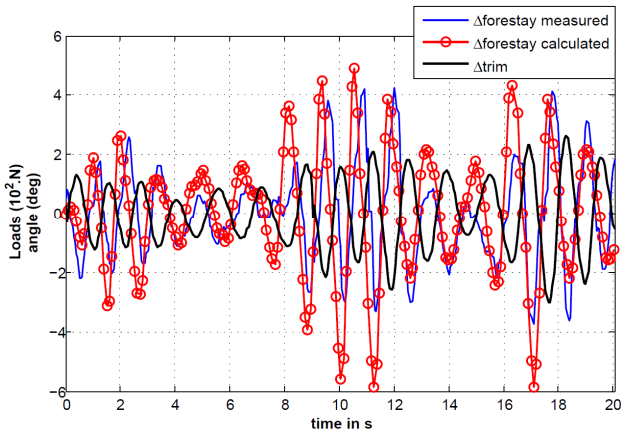


Figure 20 – Numerical and experimental comparison on the temporal variation of forestay load.

Figure 21 presents the Power Spectral Density of the simulated signal of V1portside. The PSD highlights the 2 frequencies of pitching showed in the experimental results study. Frequencies are 0.69Hz and 0.85Hz. ARAVANTI is able to simulate the influence of trim oscillation in the rig loads by modeling the amplitude variation. The model is also able to propagate precisely the frequency of a motion in the effort.

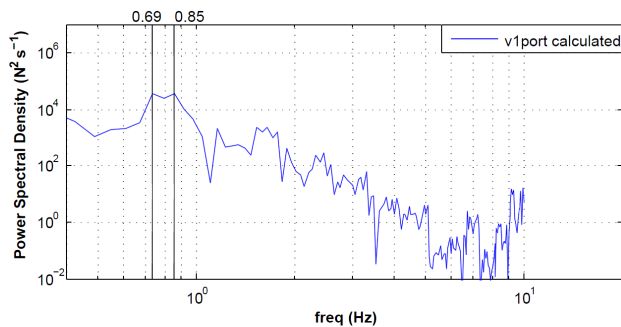


Figure 21 – Power Spectral Density of the V1portside signals with logarithmic scale.

Figure 22 presents the superposition of the hysteresis loop showed in the experimental results paragraph with the calculated loop. Forestay, main sheet and backstay load are represented depending of trim angle. The run shown corresponds to a complete period of oscillation. Simulated signals have been plotted respecting the same first run of study, in order to make a Numerical/Experimental comparison.

Calculated forestay loop has the same slope meaning

the same phase lag between forestay and trim. The phase shift due to hysteresis is well predicted. The  $\Delta$ load is the same in the calculated and measured signals.

Calculated main sheet loop has the same appearance and load variations have the same order of magnitude. For the positive values of trim –corresponding to bow diving– the main sheet load variation is a little bit under estimated.

Calculated backstay loop is in the same order of magnitude as the experimental one, but the energy in the calculated cycle is less than the measured energy.

These first unsteady simulations give interesting results regarding the ability of the model to predict the aero-elastic response of the system to a pitching forcing. The loads are well predicted, simulated in the right range of effort.

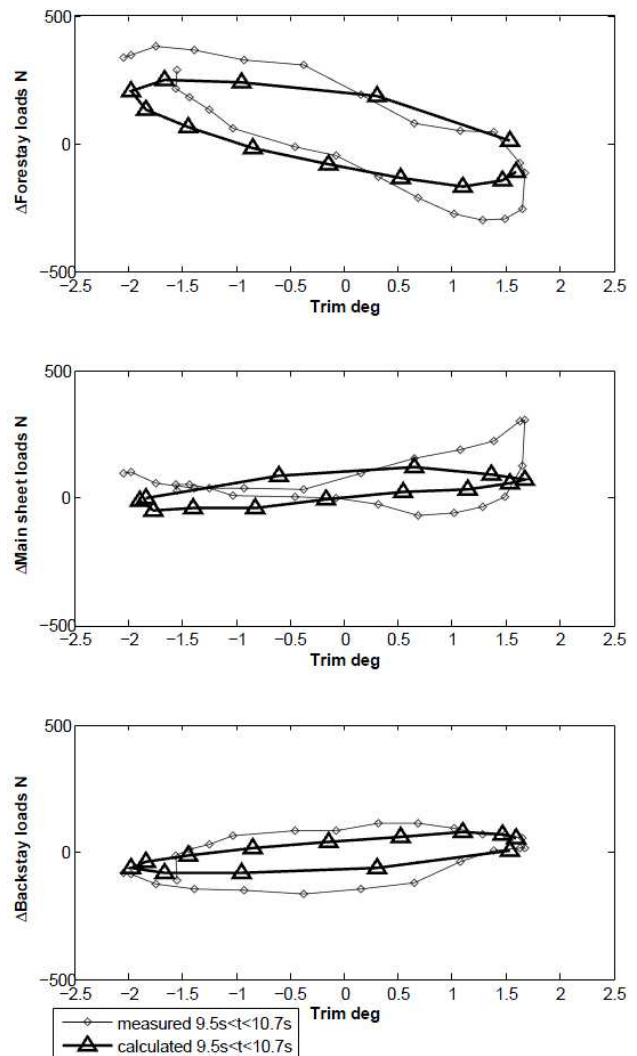


Figure 22 – Comparison of load variations with trim oscillation between the measured and calculated signals.

Unsteady simulation demands to know accurate values of all input parameters and special care is devoted to this

task., The actual rig and sails geometry and mechanical properties, and the sails trimming during the run are particularly difficult to accurately determine. The discrepancies in the experimental to numerical comparison shown for example in Figure 22 could be attributed to a rough estimation of the sail fabric behavior –scarce information on the number of yarns in the Kevlar frames of the jib.

## CONCLUSIONS

A dedicated instrumentation system has been designed on a J80 yacht to perform full scale measurement. The instrumented sail boat is developed to observe the unsteady parameters in real navigation condition. Motion, attitudes, wind, sail flying shape and loads in the rigging are recorded simultaneously.

The paper is focused on the results obtained on an upwind port tack run in head moderate swell. The influence of a dynamic forcing, pitch oscillation is highlighted in the measured loads and the wind. Amplitude of variation and over load due to oscillation are analyzed. The power spectral density of loads and apparent wind signals shows the pitching period in the parameters temporal evolution. The study and observation of the dynamic forcing conduces to try to separate the loads in two groups:

- the Structural group: boat motions have the most important influence on the tension.
- the Wind group: Wind has the most important influence on the tension.

In the Wind group, the influence of boat motion is transmitted to load by the induced wind speed created. The varying apparent wind plays the role of a system's response.

Coherence calculation shows the correlation and the phase shift between the shrouds, backstay and forestay and the trim with the loads. This phase shift induces a hysteresis effect, representing the amount of energy added or subtracted to the system by the pitching.

Post processing of sails flying shape, recorded from the top mast, is performed. Evolutions of profiles and shapes are linked to loads, confirming the tendencies observed by sailors. Flying shape is shown to be very unsteady.

The instrumented sail boat shows the major influence on loads, apparent wind and sails flying shape of a small pitch oscillation. Even in this case of rather small waves - 0.3m- over loads represent until 25% of the steady state and apparent wind is oscillating by 35%. Amplitude of variation will be way higher in open seas. Instrumentation gives data for rig and sail design and allows not applying a single security coefficient. Those results underline the importance of an unsteady model to simulate the flow and the stresses in the sail

Numerical and experimental comparisons with ARAVANTI model are presented. The preliminary steady state calculation, needed as the first step of the unsteady simulation, gives very good results. Loads are well

predicted and the computed flying shapes fit to the recorded pictures of sails.

The experimental validation of the simulation for the unsteady conditions needs more work and analysis, but the preliminary results presented here show a very similar behavior.

## ACKNOWLEDGEMENTS

This work has been done in the Voil'ENav project supported by the Naval Academy, Ecole Navale, France. The authors are grateful to K-epsilon for continuous collaboration about ARAVANTI model. Technical support from BSG Development, DeltaVoiles and Intempora is also acknowledged.

## REFERENCES

- [1] B. Augier, P. Bot, F. Hauville, and M. Durand. "Experimental validation of unsteady models for Wind / Sails / Rigging Fluid structure interaction". International Conference on Innovation in High Performance Sailing Yachts, Lorient, France, 2010.
- [2] Campbell I.M.C. "The performance of off-wind sails obtained from wind tunnel tests", R.I.N.A. International Conference of the modern yacht, 1998.
- [3] M. Caponnetto, A. Castelli, P. Dupont, B. Bonjour, PL. Mathey S. Sanchi, ML. Sawey. "Sailing yacht design using advanced numerical flow techniques". the 14<sup>th</sup> Chesapeake Sailing Yacht Symposium, Annapolis, Maryland, USA, 1999.
- [4] V. Chappin, P. Heppel. "Performance optimization of interacting sails through fluid structure coupling". International Conference on Innovation in High Performance Sailing Yachts, Lorient, France, 2010.
- [5] GF Clauss and W. Heisen. "CFD analysis on the flying shape of modern yacht sails". Maritime Transportation and Exploitation of Ocean and Coastal Resources: Proceedings of the 11th International Congress of the International Maritime Association of the Mediterranean, Lisbon, Portugal, page 87, 2006.
- [6] M. Durand, F. Hauville, P. Bot, B. Augier, Y. Roux, A. Leroyer, and M. Visonneau. "Unsteady numerical simulations of downwind sails". International Conference on Innovation in High Performance Sailing Yachts, Lorient, France, 2010.
- [7] F. Fossati and S. Muggiasca. "Numerical modelling of sail aerodynamic behavior in dynamic conditions". International Conference on Innovation in High Performance Sailing Yachts, Lorient, France, 2010.
- [8] F. Fossati, S. Muggiasca."Sails Aerodynamic Behavior

in dynamic Condition”. the 19<sup>th</sup> Chesapeake Sailing Yacht Symposium, Annapolis, Maryland, USA, 2009

[9] F. Fossati, S. Muggiasca, and F. Martina. Experimental “Database of Sails Performance and Flying Shapes in Upwind Conditions”. International Conference on Innovation in High Performance Sailing Yachts, Lorient, France, 2008.

[10] F. Fossati, S. Muggiasca, I.M. Viola, and A. Zasso. “Wind Tunnel Techniques for Investigation and Optimization of Sailing Yachts Aerodynamics”. pages 14\_16, 2006.

[11] H. Hansen, P Jackson, and K. Hochkirch. “Comparison of wind tunnel and full-scale aerodynamic sail force measurements”. 2nd High Performance Yacht Design Conference Auckland, New Zealand, 2006.

[12] S. Huberson. “Modélisation asymptotique et simulation numérique d'écoulements tourbillonnaire”. PhD thesis, Université Pierre et Marie Curie (ParisVI)- LIMSI-CNRS.

[13] D. Le Pelley, P. Ekblom, R. Flay. “Wind tunnel testing of downwind sails”, 1st High Performance Yacht Design Conference Auckland, New Zealand, 2002.

[14] Y. Masuyama, Y. Tahara, T. Fukasawa, and N. Maeda. “Database of sail shapes versus sail performance and validation of numerical calculations for the upwind condition”. Journal of marine science and technology, 14(2):137\_160, 2009.

[15] C. Rebhach. “Numerical calculation of three dimensional unsteady flows with vortex sheets”. AIAA, 16th Huntsville, paper 1978-111.

[16] H. Renzsh, K. Graf. “Fluid structure interaction simulation of spinnakers getting closer to reality”. International Conference on Innovation in High Performance Sailing Yachts, Lorient, France, 2010.

[17] Y. Roux, M. Durand, A. Leroyer, P. Queutey, M. Visonneau, J. Raymond, J.M. Finot, F. Hauville, and A. Purwanto. “Strongly coupled VPP and CFD RANSE code for sailing yacht performance prediction”. 3rd High Performance Yacht Design Conference Auckland, New Zealand, 2008.

[18] A. Scheinder, A. Arnone, A. Savelli, A. Ballica. “On the Use of CFD to Assist with Sail Design”, the 16<sup>th</sup> Chesapeake Sailing Yacht Symposium, Annapolis, Maryland, USA, 2003

[19] D. Thrasher, D. Mook, A Nayfeh, “A computer based method for analysing the flow over sails”. the 15<sup>th</sup>

Chesapeake Sailing Yacht Symposium, Annapolis, Maryland, USA, 2001

[20] I. Viola, R. Flay. “Sail aerodynamics: Full scale pressure measurement on a 24-foot sailing yacht”. International Conference on Innovation in High Performance Sailing Yachts, Lorient, France, 2010.

[21] Z. Zhang. “A flexible new technique for camera calibration”. IEEE Transactions on pattern analysis and machine intelligence, 22(11):1330\_1334, 2000.